Observation of the Sub-100 Femtosecond Population of a Dark State in a Thiobase Mediating Intersystem Crossing

Direct observation of a dark intermediate state mediating ultrafast intersystem crossing in a thiobase

Rocío Borrego-Varillas [†#], Danielle C. Teles-Ferreira [‡#], Artur Nenov[§#], Irene Conti[§#], Lucia Ganzer[†], Cristian Manzoni[†], Marco Garavelli[*§], Ana Maria de Paula[*‡] and Giulio Cerullo[*†]

[†] IFN-CNR, Dipartimento di Fisica, Politecnico di Milano, Piazza Leonardo da Vinci 32, I-20133 Milano, Italy

[‡] Departamento de Física, Universidade Federal de Minas Gerais, 31270-901 Belo Horizonte-MG, Brazil

[§] Dipartimento di Chimica Industriale, Università degli Studi di Bologna, Viale del Risorgimento 4, I-40136 Bologna, Italy

Supporting Information Placeholder

ABSTRACT: We combine sub 20-fs broadband transient absorption spectroscopy in the ultraviolet with state-of-the-art quantum mechanics/molecular mechanics simulations to study the ultrafast excited-state dynamics of the sulfur-substituted nucleobase 4-thiouracil. We observe a clear mismatch between the timescales for the decay of the stimulated emission from the bright ππ* state (≈78 fs, experimentally elusive until now) and the build-up of the photoinduced absorption of the triplet state (≈200 fs). These data provide compelling evidence that the intersystem crossing occurs via a dark state of nπ* character, which is intermediately populated on the sub 100 fs timescale. Nonlinear spectroscopy simulations, extrapolated from a detailed CASPT2/MM decay path topology of the solvated system together with an excited state mixed quantum-classical non-adiabatic dynamics, reproduce the experimental results and explain the experimentally observed vibrational coherences. The theoretical analysis rationalizes the observed different triplet build-up times of 4- and 2-thiouracil.

Thiobases[1] are DNA or RNA nucleobases where an exocyclic carbonyl oxygen is replaced by a sulfur atom. They have attracted much attention in recent years due to their biological relevance and their increasing amount of applications[2]. They have been used to improve polymerase chain reaction for DNA/RNA replication[3,4] and as cross-linking chromophores for investigation of specific interactions between nucleic acids and proteins[5,6]. Thanks to their near-unity triplet yields they have been also demonstrated as potent chemotherapeutic agents[7–9] for the treatment of some types of non-malignant hyperproliferative skin conditions and cancers. Besides their practical applications, they provide an excellent model system to understand how a single atom substitution can modify the energy relaxation pathways of the canonical DNA/RNA nucleobases. In comparison to the canonical nucleobases, thiation causes a red-shift in the absorption spectrum to the 280-400 nm range, leading to remarkable changes in the photophysics[10–16]: while in DNA/RNA monomers excited state deactivation occurs on an ultrafast timescale through a high rate of $S_1 \rightarrow S_0$ internal conversion mediated by a conical intersection (CI)[17–19], the major relaxation pathway in thiobases is via the population of long-lived triplet states through an ultrafast intersystem crossing (ISC)[13] occurring on the sub-picosecond timescale.

Over the past decade major efforts, both experimental[11–13,15,20–30] and computational[11,15,23–25,28,31–40], have been made to gain deeper understanding of the electron energy relaxation pathways and triplet state formation mechanisms in thiobases. Computational studies have suggested that the bright ππ* state relaxes on the sub-100-fs timescale by means of a CI to a dark singlet nπ* state, which acts as a doorway to the triplet manifold. Such mechanism has been proposed for a number of thiobases, including 2-thiouracil[35,39], 4-thiothymine[15], 2-thiothymine[32], 2,4-dithiothymine[33], 2-thiocytosine[23] and 6-thioguanine[31]. While the femtosecond dynamics of the triplet states formation through ISC have been measured[7,10,13,15], so far there has been no distinct experimental proof of the existence of an intermediate dark state, due to the lack of ultrafast spectroscopy data with sufficiently high temporal resolution.

Here we combine broadband transient absorption (TA) spectroscopy featuring sub 20-fs time resolution in the ultraviolet (UV) with hybrid quantum mechanics/molecular mechanics (QM/MM) state-of-the-art computational tools to study the ultrafast photoinduced dynamics of 4-thiouracil. We provide clear experimental evidence, quantitatively supported by the computational results, that ISC occurs via a dark state of nπ* character, that is intermediately populated on the sub 100 fs timescale from the bright photoexcited ππ* state.

TA measurements were carried out on a home-made pump-probe setup with sub 20 fs UV pump pulses centered at 330 nm and broadband probe pulses covering the 250-700 nm spectral range[41–43] (a description of the system and the sample preparation is provided in the Supporting Information, SI). The QM/MM computational scheme couples a state of the art *ab initio* multi-reference dynamically correlated description (CASPT2) of the 4-thiouracil with an explicit classical atomistic model (AMBER force field) of the solvent. QM(CASPT2)/MM(AMBER) static description of the potential energy surface supplemented by non-adiabatic mixed quantum-classical dynamics simulations are used to fully characterize the decay channels associated with the lowest ππ* excited state of the water-solvated 4-thiouracil. TA simulations are then performed by coupling the electronic structure computations to nonlinear spectroscopy techniques (details on the theoretical parameters provided in SI sec. 1).

Figure 1A, B shows the experimental two-dimensional (2D) maps of the differential transmission (ΔT/T) signal of 4-thiouracil dissolved in a phosphate saline buffer (PSB) solution. Immediate-

ly after the pump pulse, we observe a positive signal, which is assigned to the superposition of two bands: the tail of the ground state bleaching (GSB) band at 360 nm and a stimulated emission (SE) band peaking around 400 nm. Both the SE and GSB signals are assigned to the bright S_2 state photoexcited by the pump pulse ($\pi\pi^*$ transition).

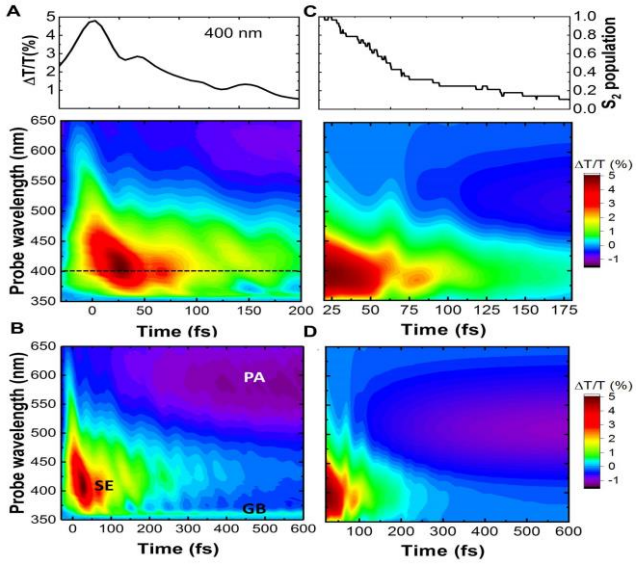

Figure 1. Experimental (panels A and B) and simulated (panels C and D) ΔT/T maps of 4-thiouracil in PBS solution. Upper panel in (A) shows the dynamics at 400 nm (dotted line in the map), upper panel in (C) shows the calculated $S_2(\pi\pi^*)$ population decay from a mixed quantum-classical molecular dynamics simulation with a set of 30 trajectories.

The SE band displays a first ultrafast decay on the sub-100-fs timescale, which is followed by the delayed build-up of a photoinduced absorption (PA) band around 600 nm on the ~500 fs timescale. The dynamics at 400 nm is shown in the upper panel of Figure 1A (dynamics at other wavelengths are shown in SI, sec. 4.3). The PA band, whose build-up has been observed in previous studies with a lower 200-fs time resolution[13], has been assigned to triplet-triplet absorption, thus providing a fingerprint of the ISC process. Following its formation, the PA band undergoes a blue-shift on the sub-picosecond timescale (Figure 2A), which is assigned to vibrational cooling of the long-lived[44,45] triplet state. At all wavelengths the ΔT/T signal is modulated by a complex oscillatory pattern that is assigned to vibrational coherences impulsively excited by the sub-20-fs pump pulse.

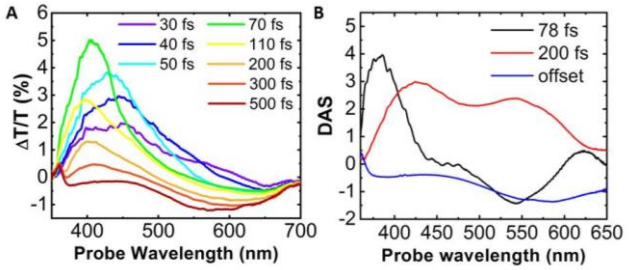

Figure 2. (A) ΔT/T spectra of 4-thiouracil at selected time delays. (B) DAS obtained by global analysis.

Our experimental data clearly show a mismatch between the decay time of the SE and the build-up time of the PA signal, thus delivering an experimental confirmation of the ISC mechanism proposed by previous theoretical works[15,23,31–33,35,36,39] that does not occur directly from the photoexcited bright $\pi\pi^*$ state but is mediated by an intermediate dark state of $n\pi^*$ character (the S_1 state). Figure 2B shows the decay associated spectra (DAS) obtained by a global fit of the data (details of the analysis are reported in the SI, sec. 4.4), revealing time constants of 78 fs and 201 fs. The 78 fs time constant (black line) is attributed to the decay of the SE band: the population of the $\pi\pi^*$ state is ballistically driven towards the $n\pi^*$ state through a CI. The 200 fs DAS band between 500 and 650 nm is associated to the subsequent triplet PA formation.

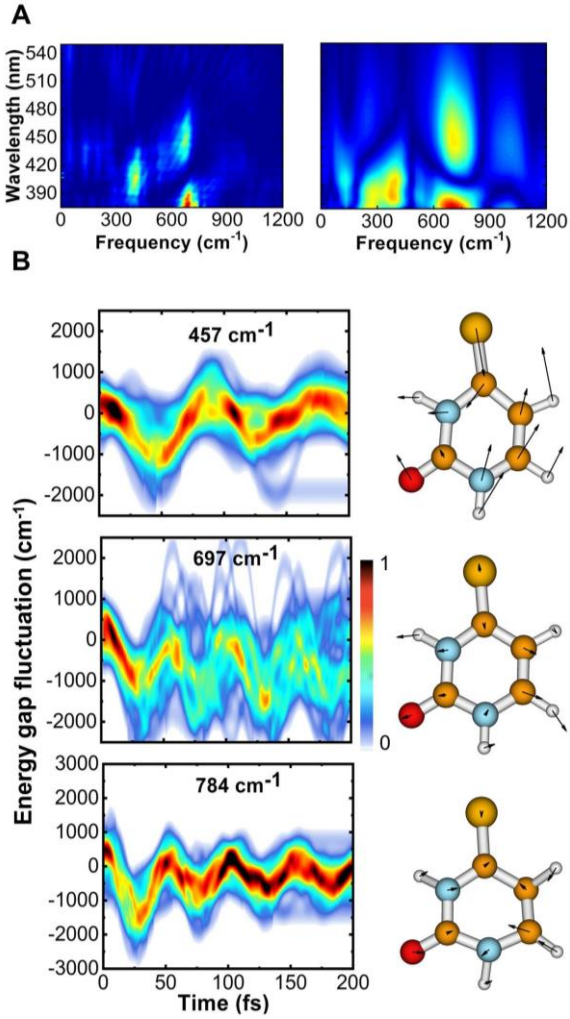

Figure 3. (A) 2D Fourier transform of the residuals of the experimental (left) and theoretical (right) ΔT/T dynamics. (B) Coherent energy gap fluctuations along selected vibrational modes at 457 cm^{-1} (ring breathing), 697 cm^{-1} (H7 and H11 hydrogen-out-of-plane (HOOP) bending) and 784 cm^{-1} (H7, H11 and H12 out-of-plane). The breathing mode gives rise to the 400 cm^{-1} peak in the 2D Fourier transforms, while both HOOP modes are responsible for the 680 cm^{-1} peaks. Intensities associated with trajectory density.

Figure 1C, D shows the simulated ΔT/T maps, constructed by means of cumulant expansion of Gaussian fluctuations using the formalism of line shape functions parametrized by analyzing the geometrical and electronic structure of the singlet and triplet manifolds (for details see SI sec. 1.4). The pump pulse populates the lowest $\pi\pi^*$ state in the Franck-Condon (FC) region. The vibrational dynamics in this bright state gives rise to intensity beats in the SE signal, whose central wavelength (400 nm) matches also the energy gap at the Min $\pi\pi^*$. A 2D Fourier analysis of the oscillatory components of the recorded (Figure 3A, left) and simulated (Figure 3A, right) spectra reveals two modes with frequencies of

680 cm^{-1} and 400 cm^{-1}. To shed light into the underlying molecular deformations we run a limited ensemble of 30 room temperature trajectories employing Tully's fewest switches surface hopping algorithm (see SI Figures 9-12, a representative trajectory depicted in the lower panel of Figure 4). A decomposition of the GS-ππ* energy gap dynamics along each trajectory into contributions from the individual normal modes within the framework of the displaced harmonic oscillator model (details in the SI, sec. 2.5) allows to identify the normal modes responsible for the coherent beatings of the SE. In particular, we observe coherent dynamics in the 457 cm^{-1} breathing mode and in two hydrogen-out-of-plane (HOOP) bending modes with frequencies 697 cm^{-1} and 784 cm^{-1} (Figure 3B), in good agreement with the experimentally observed frequencies. We associate both HOOP modes with the 680 cm^{-1} frequency in the 2D Fourier transform.

The evolution in the ππ* state leads to a sloped CI seam with the dark nπ* (Figure 4). The molecular dynamics simulations (see SI, Figures 9-12) show that ultrafast ππ*→nπ* transition is facilitated when thermal energy is inserted in the system despite the pronounced ππ*/nπ* energy gap of 1 eV at equilibrium (see SI, Figure 5). The population decay dynamics (upper panel of Figure 1C) is fitted with a time constant of 67.5 fs, in remarkable agreement with the 78 fs time constant extracted from the global analysis.

Relaxation in the nπ* state leads to a planar minimum (Min nπ* in Figure 4) which is isoenergetic with two triplet states, of ^{3}nπ* and of ^{3}ππ* nature, respectively. Hence, the nπ* state acts as a doorway for the effective population of the triplet manifold. The ^{1}nπ*/^{3}ππ* ISC is facilitated by a 150 cm^{-1} spin-orbit coupling. The longer time constant of 201 fs is assigned to the build-up of the PA from the ^{3}ππ* triplet state (Figure 1B), supported by our static computations revealing higher lying states in the triplet manifold absorbing around 600 nm from the triplet minima (in blue in Figure 4). In the simulated ΔT/T spectra (Figure 1D) these states give rise to PA around 550 nm that matches the experimentally observed 500-650 nm band (Figure 1B), as well as the corresponding band in the 200 fs DAS (Figure 2B). Instead, the 400-425 nm band present in the 200 fs DAS does not match with any computed PA either from singlet or triplet states. We note that the ^{1}nπ* state is completely dark in the probed spectral window as it exhibits no SE or PA. We assign this DAS contribution to a slower S_2 ππ* decay component, coming from vibrational modes disadvantaging the access to the nπ*/ππ* CI seam (see for example trajectories 15, 17 and 25 in the SI) or from a partial excitation of the second bright state (S_3, labeled B, blue circles in Figure 4, see also sec. 2.2 in the SI), which is expected to exhibit a delayed decay to S_2 (indicated by a dashed line in Figure 4).

Notably, we measure an ISC time in 4-thiouracil which is about two times faster compared to 2-thiouracil. Pollum et al.[13] measured a triplet build-up time of 360 fs for 2-thiouracil, in agreement with our results on 2-thiouracil showing a ≈400-fs rise time of the PA band at 600 nm (see figure S19 in the SI)[46]. According to our calculations, there are two possible explanations for this behavior. On one side, the minimum on the nπ* state in 4-thiouracil is planar in contrast to 2-thiouracil, which exhibits an out-of-plane bending of the sulfur[35,39], also characteristic for nucleobases[47,48] . On the other side, in 4-thiouracil the nπ* minimum coincides with the ISC, whereas in 2-thiouracil a barrier of ca. 0.1 eV has to be overcome[35,39].

.

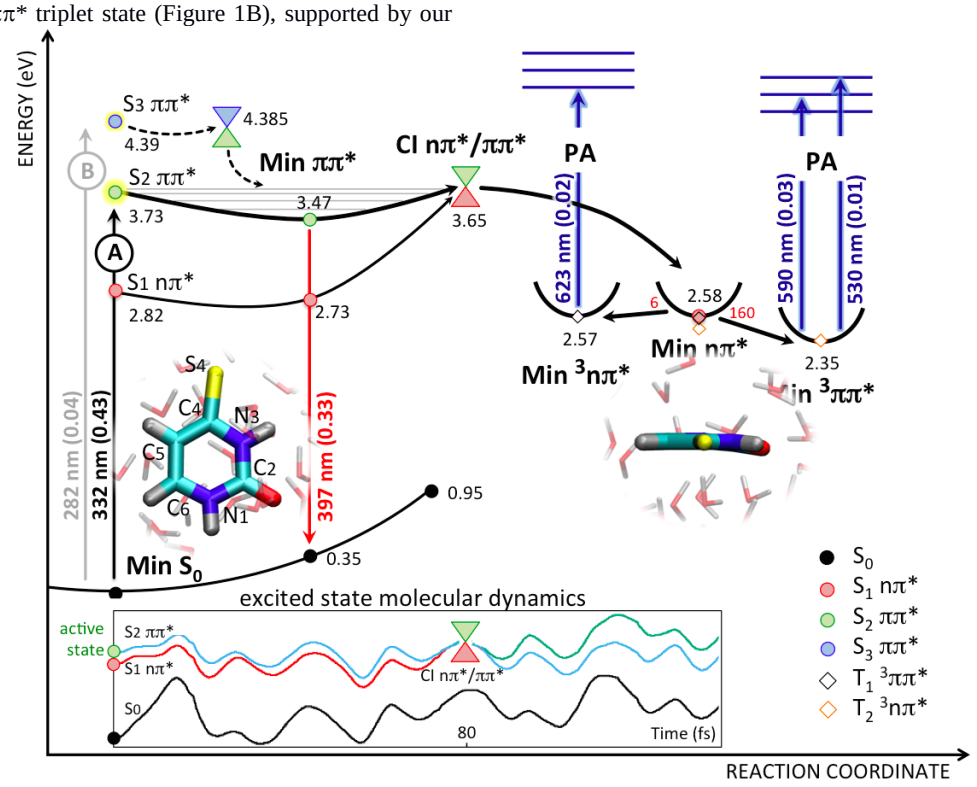

Figure 4. CASPT2/MM decay path from the lowest ππ* bright state (S_2 at the FC point) of 4-thiouracil in water. Black arrows indicate the absorption wavelength of the two lowest bright states S_2 and S_3 at the FC point. Red arrow indicates the stimulated emission out of the minimum on the lowest ππ* bright state. Blue arrows indicate the photo-induced absorption from the triplet minima, giving rise to the excited state absorption band between 500 nm and 650 nm detected after 200 fs in the transient absorption spectra (see Figure 1 B,D). Inset: a representative trajectory of non-adiabatic molecular dynamics initiated in the S_2 state (green, ππ*) and decaying to S_1 (red, nπ*) after ca. 80 fs.

In conclusion, high time resolution transient absorption spectroscopy in the UV range allowed us to observe for the first time an ultrafast (sub-100-fs) decay component in the photoinduced dynamics of 4-thiouracil following excitation of its bright ππ* state, which does not match the build-up time of the fingerprint signals of the triplet states. This is a compelling proof of the involvement of an intermediate dark ^{1}nπ* state acting as doorway to the triplet manifold. This interpretation is supported by high-level *ab-initio* static and dynamic numerical modeling, which allows us also to characterize the leading vibrational modes responsible for the experimentally observed coherences. In addition, the modeling is able to rationalize the faster triplet population in 4-thiouracil compared to its tautomer 2-thiouracil.

ASSOCIATED CONTENT

Supporting Information

Materials and steady-state spectroscopy; description of the experimental setup; transient spectra; dynamics; global analysis; coherent oscillations; details on the QM/MM protocol; details on the non-adiabatic mixed quantum-classical dynamics simulations; theoretical background of nonlinear spectroscopy; protocols for acquisition of the simulation parameters; electronic structures at representative geometries; active space orbitals; trajectory plots; normal mode analysis; Cartesian coordinates.

AUTHOR INFORMATION

Corresponding Author

* marco.garavelli@unibo.it
* ana@fisica.ufmg.br
* giulio.cerullo@polimi.it

Author Contributions

AMdP, GC, CM and MG conceived the idea. RBV and LG built the setup. DCTF, RBV and LG performed the experimental measurements. RBV and DCTF analyzed the data. IC performed the electronic structure computations. AN performed the molecular dynamics and spectroscopy simulations. RBV, DCTF, AMdP, IC, AN and GC wrote the manuscript with inputs from all the authors.

# These authors equally contributed to this work.

Notes

The authors declare no competing financial interests.

ACKNOWLEDGMENT

This work was supported by the European Research Council Advanced Grant STRATUS (ERC-2011-AdG No. 291198), the Marie Curie actions (FP7-PEOPLE-IEF-2012) and the H2020 Grant Agreement number 765266 (LightDyNAmics). DCTF and AMdP acknowledge financial support from the funding agencies Fapemig, CNPq and CAPES. We thank Dr. Stefano Santabarbara for preparing the PBS.

REFERENCES

(1) Arslancan, S.; Martínez-Fernández, L.; Corral, I. *Molecules* **2017**, *22* (6).

(2) Pollum, M.; Martínez-Fernández, L.; Crespo-Hernández, C. E. In *Top Curr Chem*; Springer, 2014; pp 245–327.

(3) Sismour, A. M. *Nucleic Acids Res.* **2005**, *33* (17), 5640–5646.

(4) Heuberger, B. D.; Pal, A.; Del Frate, F.; Topkar, V. V.; Szostak, J. W. *J. Am. Chem. Soc.* **2015**, *137* (7), 2769–2775.

(5) Meisenheimer, K. M.; Koch, T. H. *Crit. Rev. Biochem. Mol. Biol.* **1997**, *32* (2), 101–140.

(6) Favre, A.; Moreno, G.; Blondel, M. O.; Kliber, J.; Vinzens, F.; Salet, C. *Biochem. Biophys. Res. Commun.* **1986**, *141* (2), 847–854.

(7) Pollum, M.; Jockusch, S.; Crespo-hernández, C. E. **2014**, 2–5.

(8) Reelfs, O.; Karran, P.; Young, A. R. *Photochem. Photobiol. Sci.* **2012**, *11* (1), 148–154.

(9) Pollum, M.; Lam, M.; Jockusch, S.; Crespo-Hernández, C. E. *ChemMedChem* **2018**, *13* (10), 1044–1050.

(10) Reichardt, C.; Crespo-Hernaíndez, C. E. *J. Phys. Chem. Lett.* **2010**, *1* (15), 2239–2243.

(11) Reichardt, C.; Guo, C.; Crespo-Hernández, C. E. *J. Phys. Chem. B* **2011**, *115* (12), 3263–3270.

(12) Pollum, M.; Crespo-Hernández, C. E. *J. Chem. Phys.* **2014**, *140* (7).

(13) Pollum, M.; Jockusch, S.; Crespo-Hernández, C. E. *Phys. Chem. Chem. Phys.* **2015**, *17* (41), 27851–27861.

(14) Ashwood, B.; Jockusch, S.; Crespo-Hern??ndez, C. E. *Molecules* **2017**, *22* (3).

(15) Martínez-Fernández, L.; Granucci, G.; Pollum, M.; Crespo-Hernández, C. E.; Persico, M.; Corral, I. *Chem. - A Eur. J.* **2017**, *23* (11), 2619–2627.

(16) Nenov, A.; Conti, I.; Borrego-Varillas, R.; Cerullo, G.; Garavelli, M. *Chem. Phys. (Under Revis.* **2018**.

(17) Middleton, C. T.; de La Harpe, K.; Su, C.; Law, Y. K.; Crespo-Hernández, C. E.; Kohler, B. *Annu. Rev. Phys. Chem.* **2009**, *60* (1), 217–239.

(18) Crespo-Hernández, C. E.; Cohen, B.; Hare, P. M.; Kohler, B. *Chem. Rev.* **2004**, *104* (4), 1977–2019.

(19) Pecourt, J. M. L.; Peon, J.; Kohler, B. *J. Am. Chem. Soc.* **2000**, *122* (38), 9348–9349.

(20) Koyama, D.; Milner, M. J.; Orr-Ewing, A. J. *J. Phys. Chem. B* **2017**, *121* (39), 9274–9280.

(21) Sánchez-Rodríguez, J. A.; Mohamadzade, A.; Mai, S.; Ashwood, B.; Pollum, M.; Marquetand, P.; González, L.; Crespo-Hernández, C. E.; Ullrich, S. *Phys. Chem. Chem. Phys.* **2017**, *19* (30), 19756–19766.

(22) Harada, Y.; Okabe, C.; Kobayashi, T.; Suzuki, T.; Ichimura, T.; Nishi, N.; Xu, Y. Z. *J. Phys. Chem. Lett.* **2010**, *1* (2), 480–484.

(23) Mai, S.; Pollum, M.; Martínez-Fernández, L.; Dunn, N.; Marquetand, P.; Corral, I.; Crespo-Hernández, C. E.; González, L. *Nat. Commun.* **2016**, *7* (May), 13077.

(24) Mai, S.; Ashwood, B.; Marquetand, P.; Crespo-Hernández, C. E.; González, L. *J. Phys. Chem. B* **2017**, *121* (20), 5187–5196.

(25) Reichardt, C.; Crespo-Hernández, C. E. *J. Phys. Chem. Lett.* **2010**, *1* (15), 2239–2243.

(26) Reichardt, C.; Crespo-Hernández, C. E. *Chem. Commun.* **2010**, *46* (32), 5963.

(27) Yu, H.; Sanchez-Rodriguez, J. A.; Pollum, M.; Crespo-Hernández, C. E.; Mai, S.; Marquetand, P.; González, L.; Ullrich, S. *Phys. Chem. Chem. Phys.* **2016**, *18* (30), 20168–20176.

(28) Jiang, J.; Zhang, T. S.; Xue, J. D.; Zheng, X.; Cui, G.; Fang, W. H. *J. Chem. Phys.* **2015**, *143* (17).

(29) Pollum, M.; Jockusch, S.; Crespo-Hernández, C. E. **2014**, 2–5.

(30) Ashwood, B.; Jockusch, S.; Crespo-Hernández, C. E. *Molecules* **2017**, *22* (3).

(31) Martínez-Fernández, L.; Corral, I.; Granucci, G.; Persico, M. *Chem. Sci.* **2014**, *5* (4), 1336.

(32) Cui, G.; Fang, W. *J. Chem. Phys.* **2013**, *138* (4), 044315.

(33) Xie, B.-B.; Wang, Q.; Guo, W.-W.; Cui, G. *Phys. Chem. Chem. Phys.* **2017**, *19* (11), 7689–7698.

(34) Zou, X.; Dai, X.; Liu, K.; Zhao, H.; Song, D.; Su, H. *J. Phys. Chem. B* **2014**, *118* (22), 5864–5872.

(35) Mai, S.; Marquetand, P.; González, L. *J. Phys. Chem. A* **2015**, *119* (36), 9524–9533.

(36) Gobbo, J. P.; Borin, A. C. *Comput. Theor. Chem.* **2014**, *1040–1041*, 195–201.

(37) Martinez-Fernandez, L.; Fahleson, T.; Norman, P.; Santoro, F.; Coriani, S.; Improta, R. *Photochem. Photobiol. Sci.* **2017**, *16* (9), 1415–1423.

(38) Ruckenbauer, M.; Mai, S.; Marquetand, P.; Gonz?lez, L. *J. Chem. Phys.* **2016**, *144* (7), 0–8.

(39) Mai, S.; Marquetand, P.; González, L. *J. Phys. Chem. Lett.* **2016**, *7* (11), 1978–1983.

(40) Bai, S.; Barbatti, M. *J. Phys. Chem. A* **2016**, *120* (32), 6342–6350.

(41) Varillas, R. B.; Candeo, A.; Viola, D.; Garavelli, M.; Silvestri, S. De; Cerullo, G.; Manzoni, C. *Opt. Lett.* **2014**, *39* (13), 3849–3852.
(42) Borrego-Varillas, R.; Oriana, A.; Branchi, F.; De Silvestri, S.; Cerullo, G.; Manzoni, C. *J. Opt. Soc. Am. B* **2015**, *32* (9), 1851–1855.
(43) Borrego-Varillas, R.; Ganzer, L.; Cerullo, G.; Manzoni, C. *Appl. Sci.* **2018**, *8* (6), 989.
(44) Bai, S.; Barbatti, M. *Phys. Chem. Chem. Phys.* **2017**, *19* (20), 12674–12682.
(45) Taras-Goślińska, K.; Wenska, G.; Skalski, B.; Maciejewski, A.; Burdziński, G.; Karolczak, J. *J. Photochem. Photobiol. A Chem.* **2004**, *168* (3), 227–233.
(46) A detailed investigation of the 2-thiouracil ultrafast excited-state dynamics will be presented in a forthcoming contribution that is in preparation process.
(47) Pepino, A. J.; Segarra-Martí, J.; Nenov, A.; Improta, R.; Garavelli, M. *J. Phys. Chem. Lett.* **2017**, *8* (8), 1777–1783.
(48) Conti, I.; Garavelli, M. *J. Phys. Chem. Lett.* **2018**, *9* (9), 2373–2379.